Diagnostic value of stress thallium-201/rest technetium-99m-sestamibi sequential dual isotope high-speed myocardial perfusion imaging for the detection of haemodynamically relevant coronary artery stenosis

Gilles Barone-Rochette, MD, PhD,[a,b,c] Feras Zoreka, MD,[a] Loïc Djaileb, MD,[d] Nicolas Piliero, MSc,[a] Alex Calizzano, MD,[d] Jean Louis Quesada, MSc,[e] Alexis Broisat, PhD,[b] Laurent Riou, PhD,[b] Jacques Machecourt, MD, PhD,[a] Daniel Fagret, MD, PhD,[b,d] Gerald Vanzetto, MD, PhD,[a,b,c] and Catherine Ghezzi, PhD[b]

[a] Department of Cardiology, University Hospital, Grenoble Alpes, France
[b] INSERM U1039, Bioclinic Radiopharmaceutics Laboratory, Grenoble Alpes, France
[c] French Alliance Clinical Trial, French Clinical Research Infrastructure Network, Paris, France
[d] Department of Nuclear medicine, University Hospital, Grenoble Alpes, France
[e] Center of Clinical Investigations, Grenoble Alpes University Hospital, Grenoble, France

Received Aug 20, 2017; accepted Jan 4, 2018
doi:10.1007/s12350-018-1189-8

Background. **The aim of this study was to determine the diagnostic accuracy of stress thallium-201/rest technetium-99m-sestamibi sequential dual-isotope high-speed myocardial perfusion imaging (DI-HS-MPI) against invasively determined fractional flow reserve (FFR).**

Methods. **Fifty-four consecutive patients prospectively underwent DI-HS-MPI before invasive coronary angiography. Perfusion was scored visually by summed stress score on a patient and coronary territory basis. Significant coronary artery disease (CAD) was defined by the presence of ≥ 90% stenosis/occlusion or fractional flow reserve ≤ 0.80 for coronary stenosis ≥ 50%.**

Results. **FFR was measured in 69 of 162 coronary vessels, with 1.28 ± 0.56 vessels assessed/patient. Sensitivity, specificity, and diagnostic accuracy of MPI for the detection of significant CAD were 92.8%, 69.2%, and 81.4%, on a patient basis, and 83.7%, 90.4%, and 88.8% by coronary territory.**

Conclusions. **DI-HS-MPI accurately detects functionally significant CAD as defined by using FFR. (J Nucl Cardiol 2019;26:1269–79.)**

Key Words: Coronary artery disease • fractional flow reserve • SPECT • new camera CZT • dual isotope

See related editorials, pp. 1280–1283 and pp. 1284–1285

Electronic supplementary material The online version of this article (https://doi.org/10.1007/s12350-018-1189-8) contains supplementary material, which is available to authorized users.

The authors of this article have provided a PowerPoint file, available for download at SpringerLink, which summarises the contents of the paper and is free for re-use at meetings and presentations. Search for the article DOI on SpringerLink.com.

Reprint requests: Gilles Barone-Rochette, MD, PhD, Department of Cardiology, University Hospital, Grenoble Alpes, France; *GBarone@chu-grenoble.fr*

1071-3581/$34.00

Abbreviations	
CZT	Cadmium-Zinc-Telluride
DI-HS-MPI	Stress thallium-201/rest technetium-99m-MIBI sequential dual-isotope high-speed myocardial perfusion imaging
FFR	Fractional flow reserve
ICA	Invasive coronary angiography
MPI	Myocardial perfusion imaging

INTRODUCTION

Dedicated cardiac cameras with Cadmium-Zinc-Telluride (CZT) detectors have greatly improved spatial and temporal resolution that is supported by improved performance of detectors and count density, respectively.[1,2] These recent advances in nuclear myocardial perfusion imaging (MPI) have made it possible to develop a dual-isotope protocol for high-speed acquisition with image quality and radiation delivery comparable to that obtained with conventional single isotope protocols.[3] Indeed, the energy resolution of the CZT-detector allows improved separation of photopeaks from thallium-201 and technetium-99m-MIBI. With dual-isotope, the length of the procedure is decreased leading to less patient discomfort. It has also been suggested that the stronger relationship between myocardial blood flow and myocardial uptake of thallium-201 compared with sestamibi or tetrofosmin could potentially improve the ability to detect mild coronary stenosis.[4] We recently evaluated the performance of stress thallium-201/rest technetium-99m-MIBI sequential dual-isotope high-speed myocardial perfusion imaging (DI-HS-MPI) vs. invasive coronary angiography (ICA). We concluded that DI-HS-MPI was reliable at detecting or ruling out coronary artery disease (CAD).[5] However, there were limits to this previously published study, including the fact that ICA were performed for clinical indications on selected patients rather than on all patients, leading to verification bias. In addition, DI-HS-MPI diagnostic performance vs. fractional flow reserve (FFR) has not been evaluated yet. The correlation between anatomical stenosis and myocardial ischemia has been reported as being suboptimal.[6] FFR is of great value in this setting by allowing the diagnosis of CAD through the functional assessment of coronary stenosis.[7,8] The present study aimed at evaluating the diagnostic accuracy of DI-HS-MPI against invasively determined FFR.

METHODS

Patients and Study Protocol

Fifty-four consecutive patients with known or suspected CAD were recruited before clinically indicated invasive coronary angiography studies during 6 months in 2013 in our institution. All patients were referred for coronary angiography and had a high pre-test-probability, previous positive or inconclusive stress test other than MPI by the referring physician. Patients were scheduled for DI-HS-MPI within 14 days before ICA. Exclusion criteria were as follows: previously ST-segment elevation (STEMI) or non-ST-segment elevation myocardial infarction (NSTEMI), hemodynamic instability, significant valvular disease stenosis, coronary artery bypass grafting, non-ischemic cardiomyopathy, severely reduced left ventricular systolic function ($< 35\%$), and contraindications to adenosine stress. Contraindications for adenosine were asthma, second- or third-degree AV block or sick sinus syndrome without a pacemaker, systolic blood pressure less than 90 mmHg, dipyridamole-containing medications, methyl xanthenes medication within the last 12 hours prior to the test, and known hypersensitivity to adenosine. Pre-test probability of CAD was computed based on history and risk factors.[9] At the time of ICA, FFR was measured in all major patent coronary arteries with luminal diameter reduction between 50% and 90% (visual analysis) in a vessel segment ≥ 2 mm in diameter. The local research ethics committee approved the study, and all subjects gave written informed consent to participate.

CZT-Camera

Ultrafast imaging was performed using a Discovery NM 530c camera (DNM, GE Healthcare) fitted with a multi-pinhole collimator and 19 stationary CZT-detectors allowing the simultaneous acquisition of 19 cardiac views. The CZT-pixels are 2.46×2.46 mm in size and each detector consists of 32×32 pixelated CZT-elements. All stress and rest acquisition were preceded by thorough positioning of the heart within the center of the field-of-view utilizing the real-time persistence imaging tool

Imaging and Stress Protocols

Patients were instructed to discontinue beta-blocker drugs and calcium antagonists 48 hours before testing and nitrate 24 hours before testing. A bicycle exercise stress test (stepwise increments of 25 W every 2 minutes) was performed with an injection of thallium-201 at peak stress. Exercise was continued at the same effort level for an additional 60 seconds and was eventually stopped after a 6-minute recovery period at low resistance. A horizontal or down-sloping ST-segment depression ≥ 1 mm or up-sloping ≥ 1.5 mm was considered positive for ischemia. In case of inability to exercise (contraindication of bicycle exercise stress test or maximum age-predicted heart

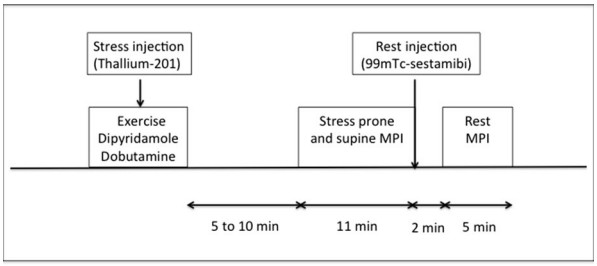

Figure 1. Dual-isotope high-speed myocardial perfusion imaging protocol.

rate (MPHR) not reached), dipyridamole (0.56 mg/kg) was infused over 4 minutes and thallium-201 was injected between 6 and 8 minutes after the beginning of dipyridamole infusion. Dipyridamole effect was reversed by systematic intravenous administration of aminophylline, usually 50 to 100 mg. For dipyridamole stress testing, patients were told to avoid caffeine-containing products for 24 hours before the test. When neither exercise testing nor dipyridamole could be used, patients were given a dobutamine stress test. Intravenous dobutamine was administered at incremental doses of 5, 10, 15, 20, 25, 30, and 40 μg/kg/min at 3-minute intervals. Patients were injected with thallium-201 at peak stress (85% of age-adjusted predicted maximum heart rate) or when chest pain, or significant ST-segment depression, or leg fatigue developed. The exercise stress test and dobutamine injection were followed by a recovery period, during which the return to normal blood pressure and heart rate was monitored. Five to 10 minutes after stress, a 5-minute supine acquisition was performed followed by a 5-minute prone acquisition. Subsequently, technetium-99m-sestamibi was injected and a single 5-minute rest acquisition was performed 2 minutes later like previously described.[3] The DI-HS-MPI protocol used is shown in Figure 1. During stress acquisition, patients were imaged in the supine and prone positions with their arms positioned over their head. The rest acquisition was acquired in supine position only. The gated-SPECT studies were performed at stress and rest in the supine position. Injected activity (IA) was adjusted for patient weight and previously described.[5] Briefly, for weights of < 80 kg/80 to 100 kg/$>$ 100 kg, thallium-201 IAs were 74/92/111 MBq (2/2.5/3 mCi) and 99mTc-sestamibi IAs were 300/370/450 MBq (8/10/12 mCi), respectively.

Analysis of Perfusion Images

Stress and rest DI-HS-MPI were semi-quantitatively scored using a 17-segment model of the left ventricle[10] and a 5-point scale (0 = normal, 1 = equivocal, 2 = moderate, 3 = severely reduced radiotracer uptake, 4 = no detectable uptake). DI-HS-MPI were visually scored by two-experienced nuclear cardiologists (D.F, A.C.) blinded to ICA data. Discordant findings were resolved by consensus. Global summed stress score (SSS), summed rest score (SRS), and summed difference score (SDS) were calculated by adding the scores for each 17 segments in the stress and rest images, respectively. SSS, SRS, and SDS were calculated also by artery territories and by segments of left ventricle. Scans were considered as normal when SSS was less than 4 for per-patients analysis and less than 2 for per-vessel territory analysis, respectively. By comparing supine and prone images, defects that changed their location were considered as artifacts,

Table 1. Baseline characteristics

Variable	*n* = 54
Age (years)	65 ± 12
Sex: males *n* (%)	41 (76)
BMI, kg m^{-2}	27 ± 5
BMI $\geq$ 30 kg m^{-2} *n* (%)	17 (31)
CV risk factors	
Hypertension *n* (%)	38 (70)
Dyslipidemia *n* (%)	32 (59)
Diabetes *n* (%)	16 (30)
Actives smokers *n* (%)	13 (24)
Family history of CAD *n* (%)	21 (38)
Peripheral vascular disease *n* (%)	5 (9)
Chronic kidney disease	12 (22)
Type of stress	
Exercice *n* (%)	27 (50)
Dipyridamole *n* (%)	25 (46)
Dobutamine *n* (%)	2 (4)
Bicycle exercise stress test	
FC maximale, bpm	143 ± 15
% MPHR	89 ± 6
PAS maximale, mmHg	179 ± 26
MPI	
Rest LVEF (%)	57 ± 9
Summed stress score *n* (%)	
0–3	20 (37)
4–8	15 (28)
$>$ 8	19 (35)
Summed rest score *n* (%)	
0–3	50 (93)
4–8	4 (7)
Cardiac medication	
Aspirin *n* (%)	45 (83)
Beta-blocker *n* (%)	30 (55)
Calcium channel blockers *n* (%)	10 (18)
ACE *n* (%)	37 (68)
ARA II *n* (%)	6 (11)
Diuretics *n* (%)	13 (24)
Statin *n* (%)	39 (72)

Data are expressed as mean ± SD or frequency (percentage)
ACE, angiotensin-converting enzyme; *ARA II*, angiotensin II inhibitor; *BMI*, body mass index; *CAD*, coronary artery disease; *ICA*, invasive coronary angiography; *LVEF*, left ventricular ejection fraction; *MI*, myocardial infarction; *MPHR*, maximum predicted heart rate; *MPI*, myocardial perfusion imaging; *PCI*, percutaneous coronary intervention

while defects remaining consistent were considered as true perfusion defects. Balanced ischemia is suspected when a reduced post-stress ejection fraction (< 45%) is noted following gated-SPECT analysis in patients with normal rest LVEF.

Furthermore, in order to assess the variability of measurements (using the SSS), MPI imaging was evaluated twice in a random order in 20 randomly selected patients (by the same observer for intra-observer variability, and by two different observers for inter-observer variability). Finally, all stress and rest imaging were scored by AC and DF for image quality using a 4-point scale: 1 = excellent (excellent quality images with no artifact), 2 = good (good quality images with total artifact score of ≤ 2), 3 = acceptable (adequate quality images with total artifact score of ≥ 3), and 4 = unacceptable (inadequate quality images with artifact severe enough to affect diagnostic quality). Image artifact was scored on a 4-point scale from 0 = none, 1 = mild, 2 = moderate, and 3 = severe.

ICA and FFR

Selective conventional ICA was performed using standard techniques (Philips Allura Xper FD10, Philips Healthcare). All patients were evaluated using quantitative coronary angiography (QCA [Vepro Computer systeme GmbH]) by two cardiologists (GB, FZ) blinded to the DI-HS-MPI results. All coronary artery stenoses were graded in at least two orthogonal views and the measurement was made in the projection showing the highest degree of stenosis. Significant CAD was defined by the presence of $\geq 90\%$ stenosis/occlusion or fractional flow reserve ≤ 0.80 for coronary stenosis $> 50\%$, cutoff in accordance with the latest recommendation.[9] FFR was performed for intermediate coronary stenoses, which were defined on the basis of visual estimation as those determining a reduction of vessel diameter between 50% and 90%.[9] FFR was measured with a coronary PressureWire-Aeris (St. Jude Medical, Minneapolis, Minnesota) at maximal hyperemia induced by the intravenous administration of adenosine (140 μg/kg/min). After maximal hyperaemia had been achieved, FFR was calculated as the ratio of the mean distal intracoronary pressure measured by the pressure wire to the mean arterial pressure measured through the coronary guiding catheter. At the end, when the pressure sensor was pulled back in the guiding catheter, both pressures were checked to exclude any drift of the transducers. To ensure correct association of the 17-myocardial segments with the subtended coronary territory, vessel dominance was used to decide if LCx or RCA supplied the inferior and inferoseptal territories. According to whether marginal or diagonal arteries supplied the anterolateral wall, either the LCx or LAD coronary arteries were defined as supplying the mid and basal anterolateral wall. If patient presented a ramus intermedius, it was defined as supplying the anterolateral wall. The large septal perforator of the LAD was defined as supplying the inferior septum.

Statistical Analysis

Statistical analysis was conducted using SPSS® version 21.0 software (SPSS Inc., Chicago, Illinois, USA). Continuous variables were expressed as mean ± one standard deviation (SD), categorical variables as counts and percentages. Analysis was performed on both a patient and coronary territory basis to determine sensitivity, specificity, and negative and positive predictive values. Sensitivity, specificity, positive predictive value (PPV), negative predictive value (NPV), and accuracy were calculated for MPI with respect to CAD detection. Receiver-operating characteristic (ROC) curve analysis was performed using the summed perfusion scores from visual analysis. For all analyses, $P < 0.05$ was considered significant. Variability was quantified computing the intraclass correlation coefficient (ICC). Inter-observer reliability for measurement of the SSS was assessed by using two-way random single-measure ICC analysis. Intra-observer and intrasubject reliability was assessed by using one-way random two-measures ICC analysis.

RESULTS

Population Study

Clinical characteristics are listed in Table 1. Mean age was 65 ± 12 years [25 to 85] and 76% were men. In this population, the pre-test likelihood of underlying CAD was 63.5 ± 18%. Indications for cardiac catheterization in this population were as follows: typical angina and pre-test-probability (> 85%) in five patients, typical angina and positive stress test other than MPI in 14 patients with intermediate pre-test-probability, atypical chest pain or dyspnea and positive stress test other than MPI in 30 patients with intermediate pre-test-probability, and chest pain and negative stress test in five patients with intermediate pre-test-probability but with strong clinical suspicion of CAD.

Invasive Coronary Angiograms

A total of 162 vessels were included in the analysis and FFR was measured in 69 out of the 162 coronary vessels with 1.28 ± 0.56 vessels assessed/patient. According to ICA + FFR data, the prevalence of significant CAD was 52%. Angiogram and FFR results are presented in Table 2. Mean FFR was 0.86 ± 0.08 (range 0.6 to 1.0), mean diameter stenosis was 58 ± 11%, and mean minimal lumen diameter was 1.8 ± 0.7 mm. Mean FFR was 0.82 ± 0.08, 0.91 ± 0.05, and 0.87 ± 0.06 on left anterior descending coronary artery (LAD), left circumflex coronary artery (LCx), and right coronary artery (RCA), respectively.

Table 2. General characteristics of epicardial stenoses

Variable	*n* = 54
Any significant CAD × per patient	28/54 (52%)
Stenosis localisation	
LMCA	0/37 (0%)
LAD	17/37 (46%)
LCx	8/37 (22%)
RCA	12/37 (32%)
Number of VD	
1-VD	19/54 (35%)
2-VD	9/54 (17%)
3-VD	0/54 (0%)
Vessels with ≥ 90% stenosis	18/162 (11%)
Vessels with CTO	2/162 (1%)
FFR positive vessels	17/162 (11%)
FFR measures	
Mean FFR on vessels with FFR < 0.80	0.74 ± 0.05
Mean FFR on vessels with FFR > 0.80	0.90 ± 0.04
FFR negative vessels	52/69 (75%)
FFR positive vessels	17/69 (25%)
QCA in vessels with FFR > 0.80	54.6 ± 9.73%
QCA in vessels with FFR < 0.80	65.4 ± 10.2%

*Significant CAD was defined by the presence of ≥ 90% stenosis/occlusion or fractional flow reserve ≤ 0.80
Data are expressed as mean ± SD or number and frequency (percentage)
CAD, coronary artery disease; *CTO*, chronic total occlusion; *LAD*, left anterior descending coronary artery; *LMCA*, left main coronary artery; *LCX*, left circumflex coronary artery; *QCA*, quantitative coronary angiography; *RCA*, right coronary artery; *VD*, vessel disease

DI-HS-MPI

Average examination time for MPI per patient was 22.4 ± 4.5 minutes. Mean SSS, SRS, and SDS were 6.4 ± 5.2, 0.7 ± 1.3, and 5.7 ± 4.8, respectively. Mean SSS was 2.7 ± 4.0, 1.5 ± 3.1, and 2.2 ± 3.0 on LAD, LCx, and RCA respectively. No patient has presented reduced post-stress ejection fraction < 45%. One hundred percent of the MPI were ranked as being of either good or excellent quality. Intra-observer and inter-observer reproducibility was high for SSS: ICC = 0.97 [95% CI 0.92 to 0.98] and 0.92 [95% CI 0.82 to 0.97], respectively. The mean injected dose for stress thallium-201 and rest technetium-99m-sestamibi was 81 ± 19 MBq (range 67 to 112 MBq) and 323 ± 41 MBq (range 263 to 455 MBq), respectively. The estimated radiation dose for dual-isotope high-speed MPI was 12.0 ± 0.8 mSv.

Table 3. Sensitivity and specificity of DI-HS-MPI vs. ICA and FFR on patient basis

DI-HS-MPI	Stenosis CAD	No stenosis CAD
Test positive	26	8
Test negative	2	18
	Se = 92.8%	Sp = 69.2%

DI-HS-MPI, dual-isotope high-speed myocardial perfusion imaging; *Se*, sensitivity; *Sp*, specificity

Diagnostic Performance of DI-HS-MPI to Detect CAD

On a per-patient based analysis, DI-HS-MPI yielded a sensitivity of 92.8% (CI 77% to 98%), a specificity of 69.2% (CI 50% to 83%), and a diagnostic accuracy of 81% for the detection of significant coronary artery stenosis (Table 3). The positive predictive value was 76.4% (CI 60% to 88%) and the negative predictive value was 90% (CI 70% to 97%). ROC analysis showed an area under the curve of 0.95 (95% CI 0.89 to 1.00; $P < 0.0001$) (Figure 2).

On a per-vessel based analysis, sensibility 83.7% (CI 68% to 92%), specificity 90.4% (CI 84% to 94%), positive predictive value 72% (CI 57% to 83%), negative predictive value 94.9% (CI 89% to 97%), and accuracy 88.8%, respectively (Table 4). Figures 3 shows a patient who presented ischemia in the anteroapical wall on myocardial by DI-HS-MPI with supine (A) and prone (B) acquisition. Figure 4 shows coronary angiogram of same patient with haemodynamically relevant coronary artery stenosis by FFR.

DISCUSSION

The results from the present study indicated that stress thallium-201/rest technetium-99m-sestamibi sequential DI-HS-MPI accurately detected the presence of significant CAD as measured using FFR.

The performances of CZT-cameras vs FFR have been less well studied than vs ICA.[11,12] However, pressure-derived FFR has become the new gold standard. To the best of our knowledge, few studies have evaluated the performance of CZT-cameras vs. FFR.[13–15] For example, Mouden et al included 100 consecutive stable symptomatic patients who were scheduled for elective FFR measurement of intermediate anatomical coronary lesions (diameter of 40% to 80%) demonstrated by recent ICA. Patients were scanned with a hybrid 64-slice SPECT/CT device (Discovery-NM-

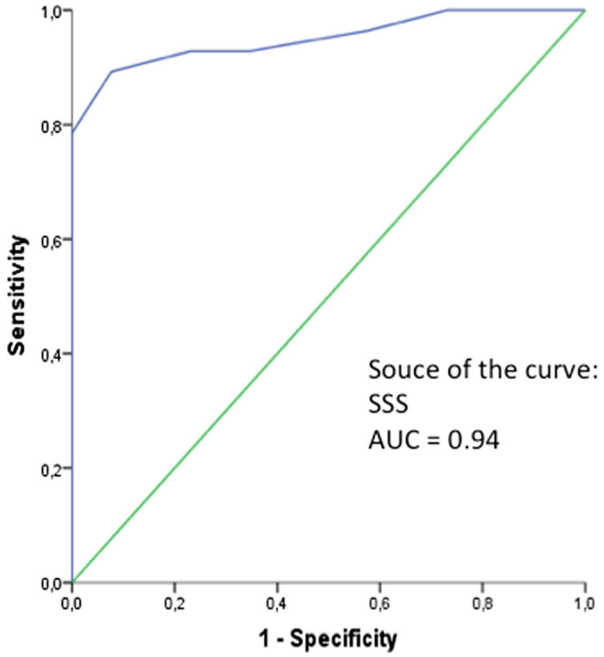

Figure 2. Receiver-operating characteristics curves derived from combined supine and prone SSS of Stress thallium-201/rest technetium-99m-sestamibi sequential dual-isotope high-speed myocardial perfusion imaging vs ICA and FFR. *FFR*, fractional flow reserve; *ICA*, invasive coronary angiograms; *SSS*, summed stress scores.

CT-570c). All patients underwent a 1 day 99mTc-Tetrofosmin study and stress/rest images were acquired 45 to 60 minutes after tracer injection. The design of this study allowed the analysis of the concordance between CZT-SPECT and FFR. The sensitivity and specificity were, respectively, 60% and 76%. The authors concluded that CZT-SPECT showed a modest degree of concordance with FFR.[13] Tanaka et al showed a high diagnostic yield of CZT-SPECT for the detection of significant coronary stenosis (diameter of 50% to 90 %) as assessed using FFR. The acquisition system was a Discovery NM 530c and the authors retrospectively studied 95 consecutive patients with suspected or known CAD who had undergone a 1 day thallium-201 study and stress/rest images. Sensitivity, specificity, and diagnostic accuracy of MPI for the detection of significant CAD were 90%, 64%, and 78%, respectively. The retrospective design accounts for the low observed specificity by referral bias, which is the main limit of this study.[14] Ben Bouallègue et al, have enrolled included twenty-three patients with known multi-vessel diseases (MVD). Dynamic-SPECT acquisitions using 99mTc-tetrofosmin at rest and after vasodilator stress were performed using a Discovery-NM-530c-camera to measure myocardial Perfusion Reserve. Due to the design only per-vessel territory analysis was available.

Table 4. Sensitivity and specificity of DI-HS-MPI vs. ICA and FFR on coronary territory basis

DI-HS-MPI	Stenosis CAD	No stenosis CAD
Test positive	31	12
Test negative	6	113
	Se = 83.7	Sp = 90.4

DI-HS-MPI, dual-isotope high-speed myocardial perfusion imaging; *Se*, sensitivity; *Sp*, specificity

With a cutoff of 2 for myocardial perfusion reserve, the sensitivity, specificity, and accuracy of regional flow ratio were, respectively, 80%, 85%, and 81% for the detection of obstructed vessels and 89%, 82%, and 85% for the detection of abnormal FFR.[15] The present study aimed at comparing the performances of DI-HS-MPI and FFR. We find excellent sensitivity at the price of more modest specificity. These results are better than those obtained with conventional-SPECT. In last meta-analysis, the sensitivity and specificity of conventional-SPECT for the detection of significant CAD were, respectively, 77% and 77% on a patient basis and 66% and 81% by coronary territory.[16] The present study demonstrates that the sensibility of DI-HS-MPI is close to 93% and favorably compares to that of CMR (Se = 90%), PET (Se = 89%) and FFR-computed tomography (Se = 89%) on a per-patient based analysis, with however a lower specificity (69% vs 87%, 84%, and 71% for CMR, PET, and FFR-CT, respectively). On a per-vessel based analysis, our results are also comparable to that obtained with these three techniques: CMR: Se = 89%, Sp = 86%; PET: Se = 87%, Sp = 85%), FFR-computed tomography: Se 83%, Sp 78%.[17–19] For stress echocardiography, the last meta-analysis confirmed a high specificity (84%) in comparison low sensibility (69%).[20]

DI-HS-MPI affords a reliable evaluation of myocardial ischemia in less than 30 minutes. Several factors may explain such positive results. The biological characteristics of thallium-201 provide optimal contrast between normally perfused and ischemic regions. DI-HS-MPI reduces acquisition times with the possibility to obtain images acquired in prone and supine positions. Image acquisition in the prone position improved the specificity for the evaluation of inferior wall abnormalities by minimizing diaphragmatic attenuation.[22]

Patients who had previously presented an STEMI or NSTEMI were excluded. Recent studies showed the influence of levels of microvascular injury to achieve hyperemia sufficient to maintain the diagnostic use of

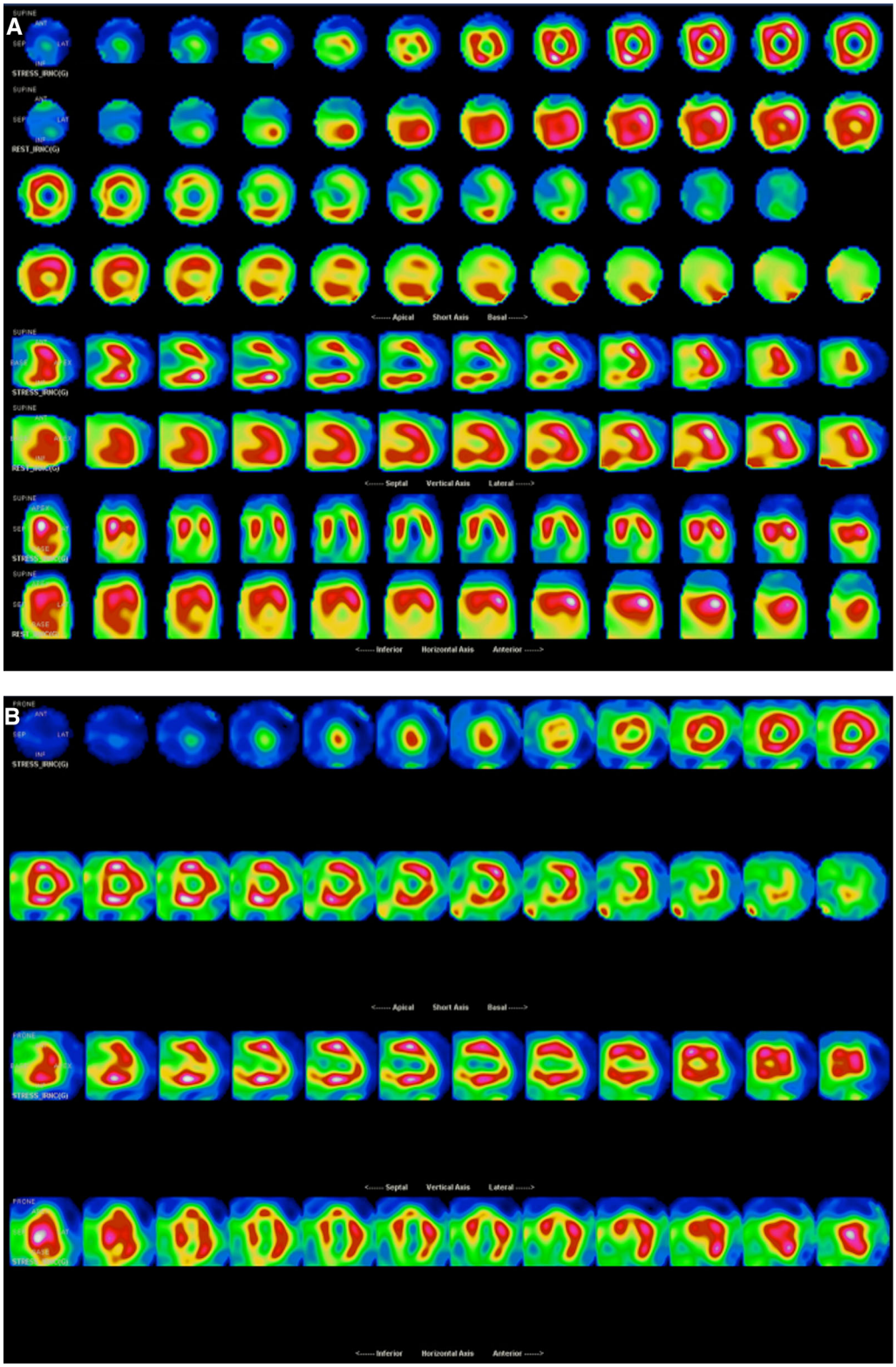

Figure 3. Panel **A** shows stress thallium-201 supine acquisition /rest technetium-99m-sestamibi supine acquisition sequential dual-isotope high-speed MPI. Panel **B** shows stress thallium-201 prone acquisition. MPI showed SSS at eight in left anterior descending coronary artery territory. *MPI*, myocardial perfusion imaging.

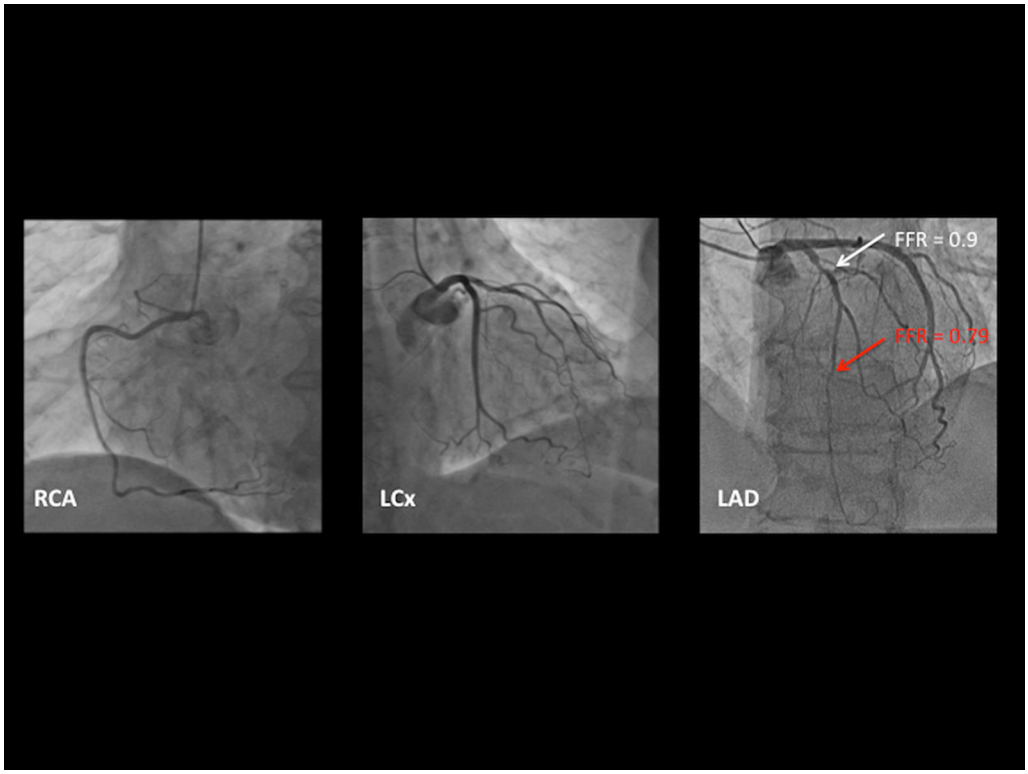

Figure 4. Coronary angiogram of same patient presented on Figure 2A and B, which shows haemodynamically relevant coronary artery stenosis on LAD. *LAD*, left anterior descending coronary artery; *LCX*, left circumflex coronary artery; *RCA*, right coronary artery.

FFR.[23] FFR reflects the hyperemic pressure gradient across a specific epicardial lesion. The pressure gradient is dependent upon the hyperemic response of the vessel distal to a stenosis. It is known that post-MI scarring reduces coronary microcirculation capacity.[24,25] In CAD, focal stenosis, diffuse atherosclerotic narrowing, and microvascular coronary dysfunction (MVCD) contribute to limit myocardial flow. FFR $\leq$ 0.80 are highly unlikely when CMVD is present.[26] Therefore, recent studies comparing magnetic resonance MPI vs. FFR excluded patients with a previous history of myocardial infarction or acute coronary syndrome.[27]

Why Use Thallium Under Stress at the Cost of Greater Irradiation? Clinical Perspectives

The use of thallium from stress MPI at the expense of a slightly higher irradiation is justified by arguments related to the quantification of ischemia. Indeed, the quantification of the ischemic burden is the cornerstone of stable coronary heart disease management.[7–9,28,29] While the physical properties of Thallium-201 might be considered suboptimal (e.g., soft tissue attenuation, long physical half life, and low energy), the kinetics of the tracer is superior to those of MIBI. Specifically, the first pass extraction fraction of thallium-201 (85%) compares very favorably with that of MIBI (65%). In comparison, ^{99m}Tc-labeled tracers are a less efficient tracer for stress imaging (extraction fraction: 65%). The lower myocardial extraction of ^{99m}Tc-labeled translates into myocardial blood flow underestimation at high flow rates induced by pharmacologic coronary vasodilatation, resulting in smaller MIBI defect size at stress in comparison to thallium-201. These consequences were clinically documented in patients with coronary artery disease.[21,30,31] While thallium-201 diagnostic superiority has not been demonstrated, the prognostic impact of better tracer kinetics may be significant due to the known prognostic value of ischemic burden assessment. The combination of improved CZT detector spatial resolution and thallium-201 superior kinetics is likely to result in improved visualization of perfusion defects due to improved detection of mild to moderate ischemia. Moreover, the improved spatial resolution of CZT detectors together with the use of thallium-201 during stress might result in improved visualization of perfusion defects due to endothelial dysfunction without any significant CAD by IA and FFR. The use of thallium-201 during stress might result in improved visualization of perfusion defects due to coronary microvascular

disease (CMVD) without any significant epicardial CAD and probably increase sensibility at the expense of specificity. Myocardial ischemia may occur in the absence of overt epicardial, atherosclerotic disease as assessed by coronary angiography due to the presence of CMVD, which has recently emerged as a major independent prognostic factor.[32,33] We have recently shown that severe CMVD might be directly observed using thallium-201 MPI in patients with no significant coronary stenosis yet elevated IMR.[34] Finally, and unlike ^{99m}Tc-labeled tracers, thallium-201 has high heart-to-liver and heart-to-spleen activity ratios irrespective of the stress method used.[4] ^{99m}Tc-labeled tracers require a significant delay between agent administration and imaging to allow for clearance of the tracer from the hepatobiliary system. In contrast, DI-HS-MPI provided a reliable evaluation of myocardial ischemia in less than 30 minutes in the present study. Such time saving allows an increase in the number of exams/day that are performed in the nuclear medicine department. The use of CZT technology for MPI is related to irradiation levels between 5 and 32 mSv depending upon population characteristics, with lower radiation doses being reported in populations with a lower prevalence of obesity.[35] In our study, 31% of patients presented with obesity.

LIMITATIONS

The study was single-centered with relatively small sample sizing. The population was free of reference bias because coronary angiography indication was not based on MPI data but on others elements thereby the use of the normalcy rate was therefore avoided. Since all patients were already referred for coronary angiography and had a high pre-test-probability, previous positive or inconclusive stress test, a selection bias was therefore specifically introduced and our data might need to be considered as preliminary. However, such methodology and sample sizing are commonly used in previously published studies evaluating MRI or CT vs. FFR.[36,37] Our data require confirmation on a larger number of patients in a multicentric study using complete invasive CMVD evaluation. Although SDS may be preferred to evaluate myocardial ischemia, a SSS > 4 was rather chosen in the present study in order to be methodologically consistent with our previously published study.[5] Such an SSS threshold has also been used by others.[38] In our center, quantitative software for image detection is not available for this technique that could improve quantification of ischemia burden. A significant proportion of CAD was made using stenosis percent at angiogram but with threshold of 90% stenosis haemodynamically relevant coronary artery stenosis is very likely. The recently developed CZT-technology provides the possibility to use a dual isotope protocol with acceptable ionizing radiation. Indeed, in a population with a mean age of 65 ± 12 years, the effective dose was 12 mSv for our study protocol with the main radiation dose coming from thallium-201. In comparison, the effective dose was 11.9 mSv for the Berman study protocol.[3] These effective doses are consistent with the average dose found in nuclear cardiology departments in North America, where SPECT is widely used for the diagnosis of CAD.[39] The possibility to use a lower dose of thallium without impairing the timeliness and quality of the images should therefore be evaluated. In this setting, and considering the superior kinetics of thallium-201 over ^{99m}Tc-labeled tracers, one might also emphasize that achieving the lowest injected dose represents a goal that should be pursued while keeping in mind both the controversial aspect of the linear, no threshold hypothesis and the patient's interest with regard to diagnostic accuracy.[40]

CONCLUSION

In patients with stable coronary disease, DI-HS-MPI can detect functionally significant CAD with excellent sensitivity, specificity, and positive and negative predictive values compared with FFR.

NEW KNOWLEDGE GAINED

We report here the first study evaluating the diagnostic accuracy of DI-HS-MPI against invasively determined FFR. DI-HS-MPI appears as a very fast and efficient technique for the detection of haemodynamically relevant coronary artery stenosis.

Disclosures

None.

References

1. Sharir T, Slomka PJ, Hayes SW, DiCarli MF, Ziffer JA, Martin WH, et al Multicenter trial of high-speed versus conventional singlephoton emission computed tomography imaging: Quantitative results of myocardial perfusion and left ventricular function. J Am Coll Cardiol 2010;55:1965-74.
2. Gimelli A, Bottai M, Giorgetti A, Genovesi D, Kusch A, Ripoli A, et al Comparison between ultrafast and standard single-photon emission CT in patients with coronary artery disease: A pilot study. Circ Cardiovasc Imaging 2011;4:51-8.
3. Berman DS, Kang X, Tamarappoo B, Wolak A, Hayes SW, Nakazato R, et al Stress thallium-201/rest technetium-99m sequential dual isotope high-speed myocardial perfusion imaging. JACC Cardiovasc Imaging 2009;2:273-82.

4. Baggish AL, Boucher CA. Radiopharmaceutical agents for myocardial perfusion imaging Circulation 2008;118:1668-74.
5. Barone-Rochette G, Leclere M, Calizzano A, Vautrin E, Céline GC, Broisat A, et al Stress thallium-201/rest technetium-99m sequential dual-isotope high-speed myocardial perfusion imaging validation versus invasive coronary angiography. J Nucl Cardiol 2015;22:513-22.
6. Toth G, Hamilos M, Pyxaras S, Mangiacapra F, Nelis O, De Vroey F, et al Evolving concepts of angiogram: fractional flow reserve discordances in 4000 coronary stenoses. Eur Heart J 2014;35: 2831-8.
7. Tonino PA, De Bruyne B, Pijls NH, Siebert U, Ikeno F, van' t Veer M, et al FAME Study Investigators. Fractional flow reserve versus angiography for guiding percutaneous coronary intervention. N Engl J Med 2009;360:213-24.
8. De Bruyne B, Pijls NH, Kalesan B, Barbato E, Tonino PA, Piroth Z, et al FAME 2 Trial Investigators. Fractional flow reserve-guided PCI versus medical therapy in stable coronary disease. N Engl J Med 2012;367:991-1001.
9. Montalescot G, Sechtem U, Achenbach S, Andreotti F, Arden C, Budaj A, et al 2013 ESC guidelines on the management of stable coronary artery disease: The task force on the management of stable coronary artery disease of the European Society of Cardiology. Eur Heart J 2013;34:2949-3003.
10. Cerqueira MD, Weissman NJ, Dilsizian V, Jacobs AK, Kaul S, Laskey WK, et al Standardized myocardial segmentation and nomenclature for tomographic imaging of the heart. Circulation 2002;105:539-42.
11. Gimelli A, Bottai M, Quaranta A, Giorgetti A, Genovesi D, Marzullo P. Gender differences in the evaluation of coronary artery disease with a cadmium-zinc telluride camera. Eur J Nucl Med Mol Imaging 2013;40:1542-28.
12. Duvall WL, Slomka PJ, Gerlach JR, Sweeny JM, Baber U, Croft LB, et al High-efficiency SPECT MPI: Comparison of automated quantification, visual interpretation, and coronary angiography. J Nucl Cardiol 2013;20:763-73.
13. Mouden M, Ottervanger JP, Knollema S, Timmer JR, Reiffers S, Oostdijk AH, et al. Myocardial perfusion imaging with a cadmium zinc telluride-based gamma camera versus invasive fractional flow reserve. Eur J Nucl Med Mol Imaging 2014;41:956-62.
14. Tanaka H, Chikamori T, Tanaka N, Hida S, Igarashi Y, Yamashita J, et al Diagnostic performance of a novel cadmium-zinc-telluride gamma camera system assessed using fractional flow reserve. Circ J 2014;78:2727-34.
15. Ben Bouallègue F, Roubille F, Lattuca B, Cung TT, Macia JC, Gervasoni R, et al SPECT myocardial perfusion reserve in patients with multivessel coronary disease: correlation with angiographic findings and invasive fractional flow reserve measurements. J Nucl Med 2015;56:1712-7.
16. Zhou T, Yang LF, Zhai JL, Li J, Wang QM, Zhang RJ, et al SPECT myocardial perfusion versus fractional flow reserve for evaluation of functional ischemia: A meta analysis. Eur J Radiol 2014;83:951-6.
17. Li M, Zhou T, Yang LF, Peng ZH, Ding J, Sun G. Diagnostic accuracy of myocardial magnetic resonance perfusion to diagnose ischemic stenosis with fractional flow reserve as reference: Systematic review and meta-analysis. JACC Cardiovasc Imaging 2014;7:1098-105.
18. Danad I, Uusitalo V, Kero T, Saraste A, Raijmakers PG, Lammertsma AA, et al Quantitative assessment of myocardial perfusion in the detection of significant coronary artery disease: cutoff values and diagnostic accuracy of quantitative [(15)O]H_2O PET imaging. J Am Coll Cardiol 2014;64:1464-75.
19. Li S, Tang X, Peng L, Luo Y, Dong R, Liu J. The diagnostic performance of CT-derived fractional flow reserve for evaluation of myocardial ischaemia confirmed by invasive fractional flow reserve: a meta-analysis. Clin Radiol 2015;70:476-86.
20. Takx RA, Blomberg BA, El Aidi H, Habets J, de Jong PA, Nagel E, et al Diagnostic accuracy of stress myocardial perfusion imaging compared to invasive coronary angiography with fractional flow reserve meta-analysis. Circ Cardiovasc Imaging 2015;8:e002666.
21. Maublant JC, Marcaggi X, Lusson JR, Boire JY, Cauvin JC, Jacob P, et al Comparison between thallium-201 and technetium-99m methoxyisobutyl isonitrile defect size in single photon emission computed tomography at rest, exercise and redistribution in coronary artery disease. Am J Cardiol 1992;69:183-7.
22. Nishiyama Y, Miyagawa M, Kawaguchi N, Nakamura M, Kido T, Kurata A, et al Combined supine and prone myocardial perfusion single-photon emission computed tomography with a cadmium zinc telluride camera for detection of coronary artery disease. Circ J 2014;78:1169-75.
23. Layland J, Carrick D, McEntegart M, Ahmed N, Payne A, McClure J, et al Vasodilatory capacity of the coronary microcirculation is preserved in selected patients with non-ST-segment-elevation myocardial infarction. Circ Cardiovasc Interv 2013;6: 231-6.
24. Marques KM, Knaapen P, Boellaard R, Westerhof N, Lammertsma AA, Visser CA, et al Hyperaemic microvascular resistance is not increased in viable myocardium after chronic myocardial infarction. Eur Heart J 2007;28:2320-5.
25. Cuculi F, De Maria GL, Meier P, Dall'Armellina E, de Caterina AR, Channon KM, et al Impact of microvascular obstruction on the assessment of coronary flow reserve, index of microcirculatory resistance, and fractional flow reserve after ST-segment elevation myocardial infarction. J Am Coll Cardiol 2014;64:1894-904.
26. Echavarria-Pinto M, Escaned J, Macías E, Medina M, Gonzalo N, Petraco R, et al. Disturbed coronary hemodynamics in vessels with intermediate stenoses evaluated with fractional flow reserve: Acombined analysis of epicardial and microcirculatory involvement in ischemic heart disease. Circulation 2013;128:2557-66.
27. Chiribiri A, Hautvast GL, Lockie T, Schuster A, Bigalke B, Olivotti L, et al Assessment of coronary artery stenosis severity and location: Quantitative analysis of transmural perfusion gradients by high-resolution MRI versus FFR. JACC Cardiovasc Imaging 2013;6:600-9.
28. Vanzetto G, Ormezzano O, Fagret D, Comet M, Denis B, Machecourt J. Long-term additive prognostic value of thallium-201 myocardial perfusion imaging over clinical and exercise stress test in low to intermediate risk patients: Study in 1137 patients with 6-year follow-up. Circulation 1999;100:1521-7.
29. Wolk MJ, Bailey SR, Doherty JU, Douglas PS, Hendel RC, Kramer CM, et al ACCF/AHA/ASE/ASNC/HFSA/HRS/SCAI/SCCT/ SCMR/STS 2013 multimodality appropriate use criteria for the detection and risk assessment of stable ischemic heart disease. J Am Coll Cardiol 2014;63:380-406.
30. Matsunari I, Fujino S, Taki J, Senma J, Aoyama T, Wakasugi T, et al Comparison of defect size between thallium-201 and technetium-99m tetrofosmin myocardial single-photon emission computed tomography in patients with single-vessel coronary artery disease. Am J Cardiol 1996;77:350-4.
31. Narahara KA, Villanueva-Meyer J, Thompson CJ, Brizendine M, Mena I. Comparison of thallium-201 and technetium-99m hexakis 2-methoxyisobutyl isonitrile single-photon emission computed tomography for estimating the extent of myocardial ischemia and infarction in coronary artery disease. Am J Cardiol 1990;66:1438-4144.

32. Camici PG, d'Amati G, Rimoldi O. Coronary microvascular dysfunction: Mechanisms and functional assessment. Nat Rev Cardiol 2015;12:48-62.
33. Bairey Merz CN, Pepine CJ, Walsh MN, Fleg JL. Ischemia and no obstructive coronary artery disease (INOCA): Developing evidence-based therapies and research agenda for the next decade. Circulation 2017;135:1075-92.
34. Djaïleb L, Riou L, Piliero N, Carabelli A, Vautrin E, Broisat A, et al SPECT myocardial ischemia in the absence of obstructive CAD: Contribution of the invasive assessment of microvascular dysfunction. J Nucl Cardiol 2017. https://doi.org/10.1007/s12350-017-1135-1.
35. Nudi F, Iskandrian AE, Schillaci O, Peruzzi M, Frati G, Biondi-Zoccai G. Diagnostic accuracy of myocardial perfusion imaging with CZT technology: Systemic review and meta-analysis of comparison with invasive coronary angiography. JACC Cardiovasc Imaging 2017;10:787-94.
36. Lockie T, Ishida M, Perera D, Chiribiri A, De Silva K, Kozerke S, et al High-resolution magnetic resonance myocardial perfusion imaging at 3.0-Tesla to detect hemodynamically significant coronary stenoses as determined by fractional flow reserve. J Am Coll Cardiol 2011;57:70-5.
37. Ko BS, Cameron JD, Meredith IT, Leung M, Antonis PR, Nasis A, et al Computed tomography stress myocardial perfusion imaging in patients considered for revascularization: A comparison with fractional flow reserve. Eur Heart J 2012;33:67-77.
38. Arsanjani R, Hayes SW, Fish M, Shalev A, Nakanishi R, Thomson LE, Friedman JD, et al Two-position supine/prone myocardial perfusion SPECT (MPS) imaging improves visual inter-observer correlation and agreement. J Nucl Cardiol 2014;21:703-11.
39. Einstein AJ, Pascual TN, Mercuri M, Karthikeyan G, Vitola JV, Mahmarian JJ, et al Current worldwide nuclear cardiology practices and radiation exposure: Results from the 65 country IAEA Nuclear Cardiology Protocols Cross-Sectional Study (INCAPS). Eur Heart J 2015;36:1689-96.
40. Siegel JA, Pennington CW, Sacks B. subjecting radiologic imaging to the linear no-threshold hypothesis: A non sequitur of non-trivial proportion. J Nucl Med 2017;58:1-6.